Instrument Deployment Testbed: For Planetary Surface Geophysical Exploration

Ashitey Trebi-Ollennu, Arturo L. Rankin, Yang Cheng, Kam S Tso, Robert G Deen,
Hrand Aghazarian, Eric A. Kulczycki, Robert G Bonitz, and Leon Alkalai

Jet Propulsion Laboratory
4800 Oak Grove Dr.
Pasadena, CA 91109
818-354-4605
ashitey@jpl.nasa.gov

Abstract—This paper describes a high fidelity mission concept systems testbed at JPL that was used to support the InSight (Interior Exploration Using Seismic Investigations, Geodesy, and Heat Transport) mission concept study. The InSight mission would conduct geophysical exploration of Mars' interior using three instruments 1. SEIS seismometer monitors seismic activity and tidal displacements; 2. RISE X-band radio Doppler tracking experiment measures rotational variations; and 3. HP3: Heat-flow and Physical Properties Probe determines the geothermal heat flux. CNES contributes SEIS and DLR contributes HP3. The measurements from these instruments would yield information about processes that occurred during the initial accretion of the planet, the formation and differentiation of its core, crust, and mantle, and subsequent evolution of its interior. The SEIS and HP3 instruments will be deployed to the surface of Mars using a robotic arm similar to the robotic arm used on the Mars Phoenix Lander mission and operational experience inherited from Phoenix and MER. The SEIS and HP3 will be monitored every three hours for one Mars year, with no ground-in-the-loop interaction required. InSight was one of three proposed missions selected by NASA Discovery Program in May 2011 for funding to conduct preliminary design studies and analyses. InSight was selected in August 2012 as the 12th mission in the NASA Discovery Program.

TABLE OF CONTENTS

1. INTRODUCTION

InSight a geophysical investigation of Mars, was one of three proposed missions selected by NASA Discovery Program in May 2011 for funding to conduct preliminary design studies and analyses under NASA's Discovery Program. InSight was selected in August 2012 as the 12th mission in the NASA Discovery Program. InSight builds on spacecraft technology used in NASA's highly successful Phoenix lander mission, which was launched to the Red Planet in 2007 and determined water existed near the surface in the Martian polar regions.

This paper describes how the InSight mission preliminary design studies and analyses team used the planetary surface geophysics instrument deployment testbed to evaluate the performance of key design parameters for the first planetary surface instrument deployment mission concept. The testbed also enabled early risk reduction activities in Phase A of a NASA project life cycle. In addition, the instrument deployment testbed for planetary surface geophysical exploration provided a unique infrastructure that enabled the InSight mission preliminary design study team to configure and demonstrate end-to-end surface operations using existing JPL mission operations and ground support tools, Lander, robotic arm, stereo algorithms, flight software, and soil simulant (regolith), in a high fidelity functional testbed. The planetary surface geophysics instrument deployment testbed was used to demonstrate the end-to-end surfaces operations of the InSight mission to the NASA reviewers at a site visit in May 2012.

InSight flight system is a close copy of the Mars Phoenix Lander and comprises of a Lander, cruise stage, heatshield and backshell. The Lander subsystem (shown in Figure 1) is the core of the flight system and controls all functions throughout the mission phases. The InSight Instrument Deployment System (IDS) (shown in Figure 1) and science payload with accompanying auxiliary peripherals are mounted on the Lander. The IDS comprises the IDA (Instrument Deployment Arm), IDC (arm mounted Instrument Deployment Camera), ICC (lander-mounted Instrument Context Camera), and control software. InSight IDA will be refurbished MSP01 flight arm currently in storage at JPL. The IDA has one degree of yaw joint (shoulder azimuth), and three pitch joints (shoulder elevation, elbow, wrist). The MSP01 IDA includes a legacy scoop, which is not required by InSight IDA for nominal instrument deployment operations.

The InSight end-effector is a magnetic grapple on a 20 cm umbilical. A permanent rare-earth magnet provides the lifting force and redundant field-cancelling electromagnets are used for the release function. The grapple release is triggered by ground command and the design is robust against unexpected power loss because power is required for release.

The IDA workspace (shown in Figure 1) is defined by its 1.9m reach and it is large enough to assure instrument
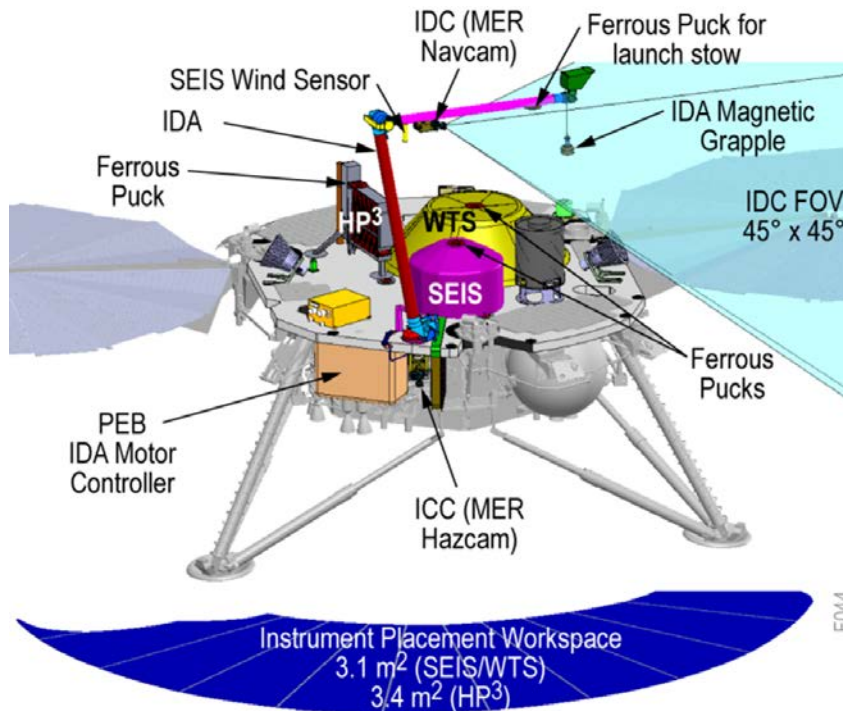
Figure 1- CAD model of the InSight Lander, Instrument Deployment System and Science Payload

Phoenix flight system testbed Lander deck populated with mass and volume equivalent mockup models of SEIS, WTS, HP3, RISE and UHF antenna

Deployed mockup mass and volume equivalent mockup models of SEIS,WTS and HP3 in the sandbox.
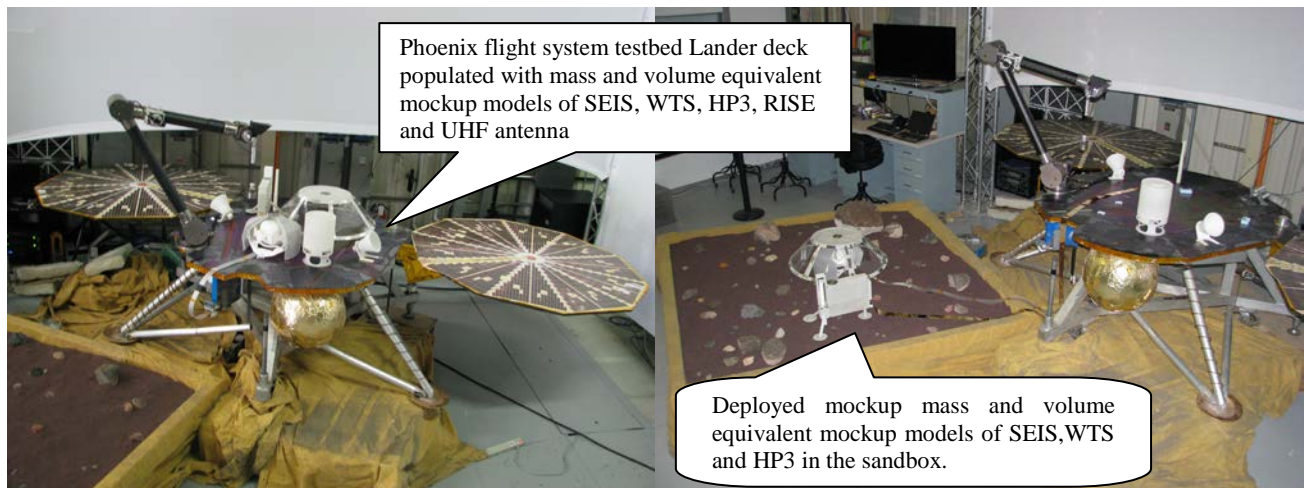
Figure 2 - Planetary surface geophysics instrument deployment testbed

placement options for a wide range of rock distributions. The IDA has a lift capacity to place the geometric centers of the 7.8-kg SEIS and 6.3-kg. WTS within a 3.1-m^2 workspace; the 2.1-kg HP3 can be placed within a 3.4-m^2 area.

The IDC is mounted on the IDA facing the end effector as shown in Figure 1. The IDC has 45°x45° FOV (field of view). The IDC is used to acquire stereo pairs of the IDA workspace to create DEM, a technique used on the Phoenix mission as well as visual confirmation of instrument deployment steps. The IDC is also used for engineering assessment of the Lander post landing, to acquire images of solar arrays, payload deck, and instruments. The ICC, a single eye camera is mounted 45° below horizontal on the underside of the payload deck. The ICC has a 124° FOV and provides an unobstructed view of the IDA deployment workspace.

SEIS, RISE and HP3 sensor heads are mounted on the Lander deck as shown in Figure 1. In addition, a free standing Wind and Thermal Shield (WTS) is mounted on the Lander deck. The WTS will be placed over the SEIS post surface deployment (see Figure 2). The WTS isolates the seismic sensors from direct wind force, leaving only indirect coupling through the ground from wind-induced Lander motion etc. The SEIS, RISE and HP3 electronics are located inside the Lander thermal enclosure. A 3m long, and

4.5cm wide tether connects the SEIS sensor head to the SEIS electronics box in the Lander thermal enclosure. The 3m SEIS tether is housed in a tether box underneath the Lander.

The HP3 sensor head has two tethers, a 3m engineering tether that connects the deployed HP3 sensor head to the HP3 electronics located inside the Lander thermal enclosure. The second is a science tether connected to the heat probe directly.

The planetary surface geophysics instrument deployment testbed configuration for InSight (shown in Figure 2) consisted of the Phoenix flight systems testbed Lander, COTS IDA, COTS IDC, COTS prototype of magnetic grapple end-effector, a sandbox with Mars regolith simulants including size distribution of rock, mass and volume equivalent mockup models of the SEIS, HP3, WTS and other Lander deck elements shown in Figure 2. The testbed Command & Data Handling (C&DH) includes a COTS Payload Interface Module computer used to emulate the flight hardware interfaces and software drivers for the payload elements of the surface mission. The C&DH configuration for the testbed enabled us to rapidly demonstrate end-to-end surface operations leveraging JPL heritage mission operations and ground support tools.

In the following sections we will provide a brief description of the planetary surface geophysics instrument deployment testbed subsystems configuration for InSight, present systems level end-to-end surface operations test results, and draw some conclusions.

2. SYSTEM DESCRIPTION

Prototype COTS IDA (Robotic Arm)

A custom four degree-of-freedom (yaw, pitch, pitch, pitch) arm was designed and built for the instrument deployment testbed [1]. The kinematics of this arm is shown in Figure 3. The arm allows the SEIS, WTS, and HP3 to be lifted off the Lander deck and placed on the Martian surface. A cross-sectional view of the wrist joint can be seen in the Figure 4. This joint is representative of the basic actuator design throughout the arm. All of the joints comprise of an 80:1 harmonic drive on the output driven by a 1.5:1 helical gear pass, then a multi-stage (3 or 4 stages) planetary gear and brushless DC motor. All of the motors also have a safety brake (power to disengage) and incremental optical encoder on the input 4 side. There is also a single turn absolute optical encoder on the output of the joint. The encoder mount also serves as a grease trap for the helical pass lubrication. The structure of the arm is sized to take the ratchet torque of the harmonic drives. In this way, the harmonic drives act as mechanical fuses in the event of a severe overload event.

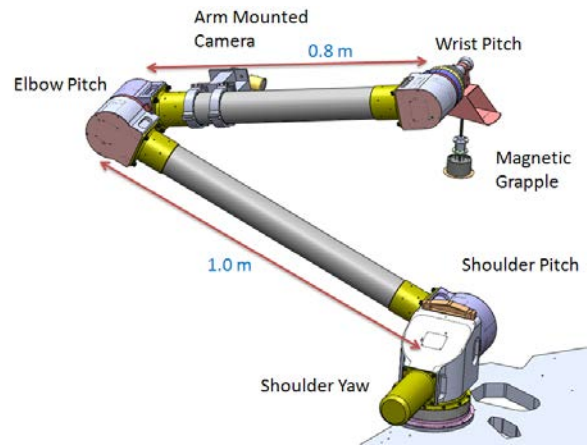Moving hard-stops allow each joint to travel more than +/- 180°.

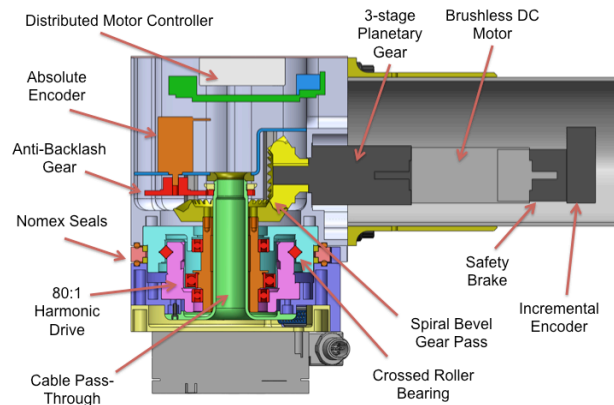**Figure 3- The 4-DOF COTS IDA**

Figure 4 - Cross-Sectional View of the Wrist Pitch Joint.

In order to encode the full range of motion with the single-turn absolute encoder, a slightly negative gear reduction is added between the joint output and the encoder. This gear pass includes an anti-backlash gear on the encoder.

Distributed motor controllers are used throughout the robotic arm and each controller is co-located with its associated joint. Distributed control significantly reduces the bulk diameter of wire harness traveling down the arm. The center of both the harmonic drive and the helical output gear are hollow, allowing for the harness to pass coaxially through without risk of chopping. This scheme greatly reduces the complexity of hardware required to protect the wire harness. Typical space robotic arms have relied on ribbon flex cable and spiral service loops to achieve the desired range of motion on the joint. This design is more consistent with industrial robotic arm design and allows for the use of a traditional round-wire harness, which is significantly less expensive and much easier to install and repair.
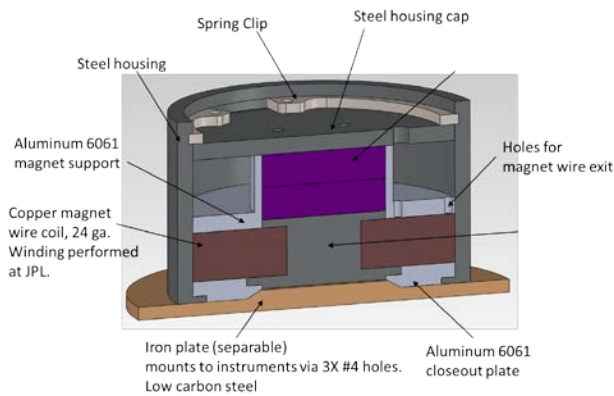
Figure 5 - Cross-Sectional View of COTS Prototype Magnetic Grapple.

Figure 6 - COTS prototype magnetic grapple on a 20 cm umbilical lifting a mass and volume mockup model of SEIS off the Phoenix flight systems testbed Lander.

The magnetic grapple [2 NTR] shown in Figures 5 and 6 is designed to lift the SEIS, WTS, and HP3 and safely place each on the Martian surface at maximum tilt of 15 degrees. The tether utilized in this design is both mechanical and electrical by design as it provides the strength to lift instruments and send power to the internal electro-magnetic coils. The grapple uses a permanent rare-earth magnet as the lifting force. Using the IDA the grapple is mated with a steel interface plate on the instrument. The interface plate is designed such that the magnet will self-align with the interface plate. Redundant field-cancelling electromagnets are used for the release function in combination with IDA motion to separate the grapple from the instrument. Grapple release is triggered by ground command and the design is robust against unexpected power loss because power is required for release. The COTS prototyped magnetic grapple was tested extensively in the testbed and demonstrated successfully at the NASA reviewers' InSight site visit in May 2012.

Software Architecture

The planetary surface geophysics instrument deployment testbed software is divided into the onboard flight software and the ground support utilities [1]. It is based on the JPL ATHLETE System Architecture Platform (ASAP) [3]. ASAP is a framework for real-time embedded software based on hierarchical state machines (HSMs) and message-passing. It is a direct extraction from the ATHLETE robot flight software, which has extensive heritage from the Mars Exploration Rover (MER) mission [4].

Under the ASAP architecture the software is broken into modules, each of which provides a specific service. Modules are themselves broken into objects, each of which encapsulates an area of responsibility. Objects are implemented in C++ as hierarchical state machines, are loosely coupled, and communicate with each other using asynchronous messages to request services and deliver data [3]. Figure 7 shows the software modules composing the planetary surface geophysics instrument deployment testbed software. The ASAP modules are utilized without change. The other modules are developed for the COTS IDA and COTS IDC control. The flight software and ground utilities run on separate computers on top of the Linux operation system. Realtime commands are by the RECV module and are dispatched by the CMD module as received, and several can be active at the same time. A command sequence is a list of commands that are pre-validated and then run one at a time. There can be multiple SEQ engines, so multiple sequences can be active at one time.
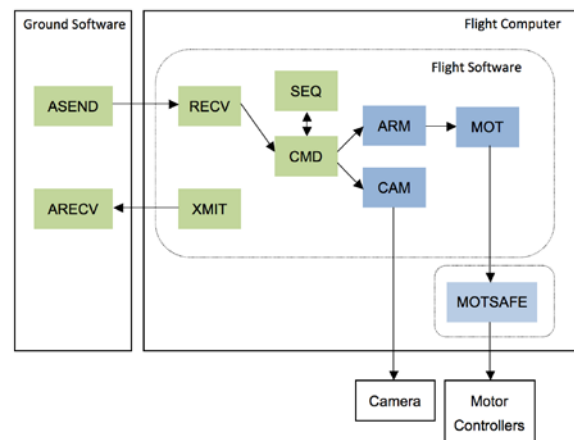

Figure 7 - Onboard software architecture

The ARM module implements the forward kinematics and inverse kinematics of the arm. It accepts both arm commands in both the joint space and Cartesian space for relative or absolute motions. Cartesian commands can be specified in tool or lander frame. The arm motions are decomposed into a set of via points sent to the MOT module. When the MOT module receives motion requests it starts all motors at the same time and scales the velocity limits so that nominally all motors will complete motion at the same time. If a fault is detected on any motor in the

request, MOT stops all motors in that request. Active motion requests can be updated (go to the next via point) or stopped by the ARM module. A callback function is passed with the MOT request so that the ARM module receives and monitors arm motion continuously. Motor motions are translated into Elmo controller commands which are send to the MOTSAFE module. The MOTSAFE module, runs as a separate process, is a small trustworthy piece of software that is rarely changed. It talks to the Elmo motor controllers by way of a CANbus. MOTSAFE detects many types of errors, including loss of communication with the flight software and motor controllers, and invalid commands from the flight software. When error is detected, it ramps down the motors and closes the brakes. MOTSAFE can be run in simulated mode emulating the actions of the Elmo controllers and motors. This enables the development of the flight software with the need of the hardware transparently.

The CAM module accepts commands to capture camera images and saves them to the Image Store. It subscribes for continuous update of arm state data so that the current pose of the arm can be written to the image metadata. The ground support utilities include ASEND and ARECV. ASEND is a simple tcl utility that accepts, parses, and validates user input of commands and sends it to the flight software over a TCP/IP socket. The ARECV is a console program that accepts channelized telemetry data and displays them on the console.

The Rover Sequencing and Visualization Program (RSVP) is also integrated with the testbed software [5]. The RSVP HyperDrive provides 3D visualization of the COTS IDA workspace and the terrain models generated by MIPL based on the images captured by the CAM module. The InSight Lander and IDS models are integrated in the testbed version of RSVP as shown in Figure 14. RVSP enables detailed simulation of the robotic arm motion, which is driven by the ground version of the ASAP software described earlier.

COTS IDC

The COTS IDC is mounted to the COTS IDA. Figure 1 illustrates the placement of the IDC on the robotic arm. The COTS IDC is side mounted to a custom built bracket that extends the COTS IDC 0.1935 meters to the side of link 2 with an adjustable camera tilt angle. The COTS IDC tilt angle is fixed at 20° down such that the robotic arm end effector is in the middle of the horizontal field of view (HFOV) but at the upper edge of the vertical field of view (VFOV). In this configuration, the camera can be used to image the Lander deck, the payload in situ instruments during deployment, or the terrain that is within the robotic arm's workspace. The COTS IDC is a monochrome Point Grey Research Flea2 camera, configured such that the output resolution, FOV, and dynamic range are similar to the Mars Exploration Rover (MER) navigation cameras [6]. The native image resolution (2448x2048 pixels) is subsampled and cropped onboard the camera such that the output resolution is 1024x1024 and the pixel pitch is 6.9μm.

The camera dynamic range is 12 bits per pixel. A 8mm focal length lens was selected such that the FOV is 47.65°x47.65° and angular resolution is 0.8122 mrad. To minimize changes to existing visualization, image mosaic, and terrain mesh ground tools, COTS IDC image data products are saved in the same format as the MER navigation cameras [6]. Because the IDC is side mounted, the IDC images are rotated counterclockwise 90° prior to saving them in image data products.

The COTS IDC was calibrated using a planar target having a fixed pattern of 100 dots with known diameter and spacing. Nine COTS IDC images were acquired with the target positioned to cover portions of the field of view at a range of distances from the camera. A sample calibration image is shown in Figure 8. The calibration imagery was processed with JPL dot finding software that generates a CAHVOR camera model [6]. The CAHVOR camera model precisely describes how 2D image coordinates map to 3D space, and vice versa. The camera model residual was 0.2576 pixels. The CAHVOR camera model saved on the InSight gateway computer is expressed in the camera coordinate frame. However, at each COTS IDC imaging position, the CAHVOR camera model is transformed into the payload frame by performing forward kinematics using the robotic arm joint angles. The transformed CAHVOR camera model is saved in an image data product with the corresponding image.

Two types of imaging sequences have been constructed for the InSight configured instrument deployment testbed; mesh and mosaic sequences. Both types of imaging sequences contain three commands for each imaging position; an absolute or relative arm motion command, a short time delay to allow post-motion arm vibration to subside, and the image capture command. The image capture command allows the user to specify full resolution, subframing, subsampling, pixel bit depth, and auto or manual exposure mode.

Mesh sequences are structured to capture images of the robotic arm's workspace in several tiers, starting with an inner tier close to the base of the lander and moving progressively outward. Only the COTS IDA azimuth (a0) joint angle is changed within a tier. To move from one tier to the next, COTS IDA elbow joint angle (a2) is changed. A mesh sequence acquires pairs of images with substantial overlap, accomplished by making small changes to COTS IDA azimuth joint angle (a0). Mesh sequence pairs of images are saved as left eye and right eye image data products and are used by a ground tool to perform stereo ranging. The range data from each pair of images is combined into a composite point cloud and used to generate digital elevation map, also called a terrain mesh.

A mosaic imaging sequence also acquires tiers of images, but they are not acquired in pairs and the overlap between images is minimal. Mosaic images are stitched together in a single panorama image by a ground tool. Each image

capture command in a sequence specifies if the image should be saved as a single eye COTS IDC image (for a mosaic), left eye IDC image (for a mesh), or right eye COTS IDC image (for a mesh).
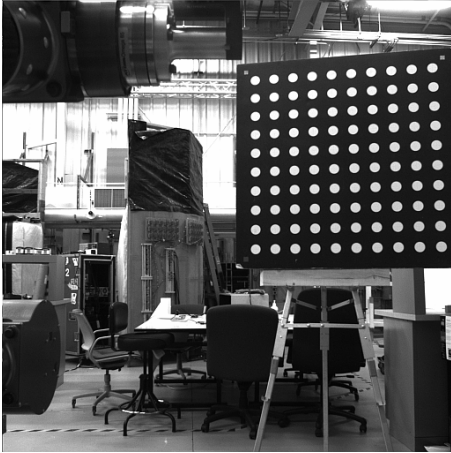

Figure 8 COTS IDC image with the calibration target in the FOV. The end effector scoop is rotated up out of the FOV and the magnet is manually placed on top of the scoop.

Figure 9 illustrates stereo disparity images from processing 16 pairs of images of a portion of a sandbox at half resolution using a SAD5 1D stereo correlator [7]. The LSOT arm was used for this data set [1]. Note that there are small spots with loss of data (beyond where the LSOT arm occludes the terrain). This is due to inevitable errors in measuring the camera's pose in the payload frame. Higher data density could be achieved by performing 2D stereo correlation with a ground tool or performing feature detection and motion estimate between the image pairs prior to 1D stereo correlation, both at the cost of higher processing time.
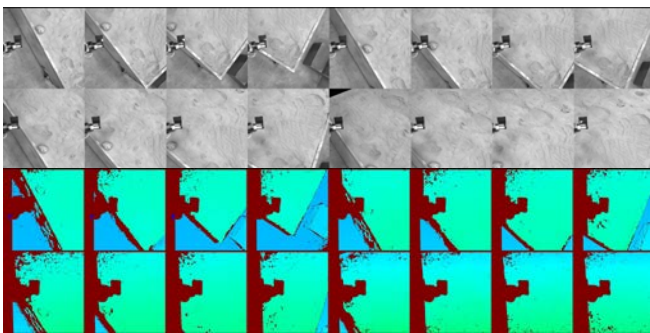

Figure 9. Sixteen rectified left eye images of a sandbox and the corresponding disparity images using a 1D SAD5 correlator. Images were processed at half resolution (512x512). Images were captured using the LSOT arm in 4 tiers, 4 pairs of images per tier, denoted 4x4.

In this data set, the arm azimuth angle (a0) was changed 10° between pairs of images. The change in the camera pose between image pairs in each tier was repeatable. After transforming the camera model at each imaging position (by performing forward kinematics using the robotic arm joint angles), the average change in right camera position with respect to the left camera for the 16 stereo image pairs was 0.000435 meters. The average change in the right camera boresight unit vector with respect to the left camera was (0.000090, 0.000574, -0.000031).

As shown in Figure 10, given the camera height H from the planetary surface, the camera FOV θ, and the desired percent overlap in stereo pairs of images, one can calculate the required stereo baseline B and the change in the arm azimuth angle a0 between image pairs (equation 1). After acquiring an image pair, the optimal change in a0 to the start of the next image pair in a tier or the optimal change in a2 to the start of a new tier can be determined experimentally, starting with large values and reducing them until there are no gaps between stereo regions. As shown in Figure 11, we implemented a spreadsheet that displays the overlap in stereo regions, given joint angles for each imaging position. This tool was used to speed up the process of finding the optimal change in a0 between image pairs and change in COTS IDA elbow joint angle (a2) between tiers.
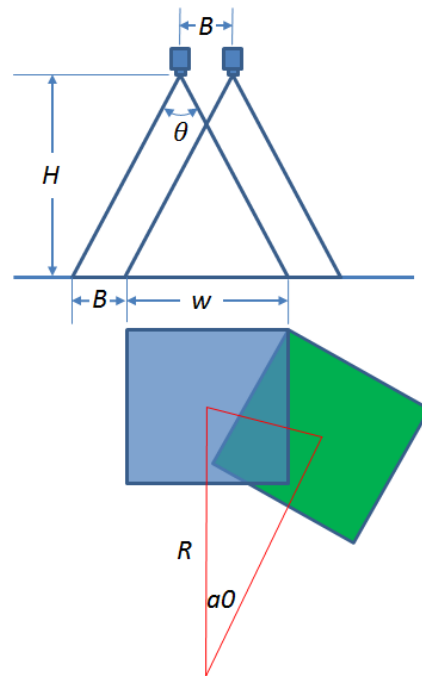

Figure 10 The azimuth angle *a0* between a stereo pair of images as a function of image overlap *w* and the reach of the arm *R* in the payload *xy* plane.

$$w = 2H \tan\left(\frac{\theta}{2}\right)[\% overlap]$$

$$B = 2H \tan\left(\frac{\theta}{2}\right)[1 - \% overlap] \qquad (1)$$

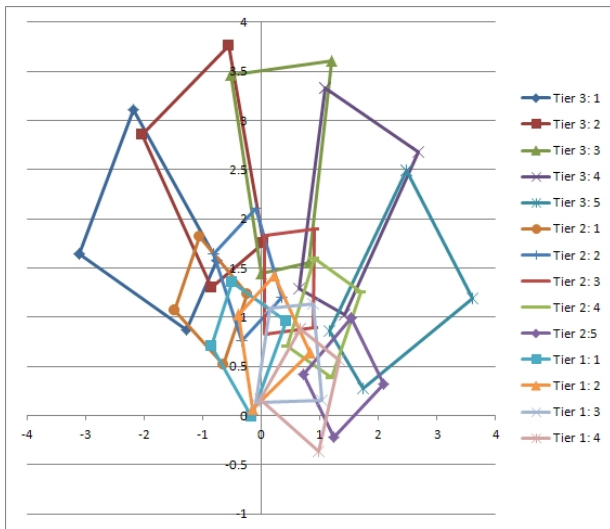$$a0 = 2\tan^{-1}\left(\frac{w}{w + 2R}\right)$$

Figure 11 Predicted overlap between 4x4 stereo regions in a birds-eye view of a level surface. A spreadsheet was developed that inputs arm joint for a set of stereo pairs of images and outputs the footprint of each stereo pair of images on a level surface.

Ground Processing of COTS IDC Images

The Ground Data System (GDS) for imaging for the testbed was created and managed by the Multimission Image Processing Lab (MIPL) at JPL. The system was based on the LSOT (Lunar Surface Operations Testbed) GDS used for the MoonRise proposal in 2011 [1] with minor modifications. That system was in turn based on the Mars Exploration Rover (MER) operational system [8]. The planetary surface geophysics instrument deployment testbed system thus benefitted from significant heritage, which greatly reduced the time for implementation. Figure 12 shows an overview of the system and the inheritance.
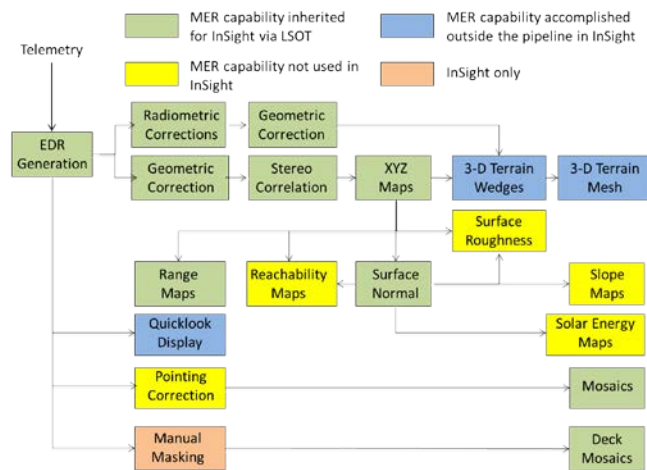

Figure 12 MIPL Image Product Pipeline for the instrument deployment testbed

The system starts when it receives image data products (telemetry) from the testbed spacecraft flight system. These are converted into Experiment Data Records (EDR's),

which are the raw image data products in a form usable to ground tools. From these EDR's, Reduced Data Records (RDR's) are created. These RDR's contain results from processes such as geometric rectification, stereo correlation, XYZ and surface normal generation. The RDR's are then processed into mosaics (images of the workspace and deck) and meshes (terrain models). MIPL visualization tools, primarily xvd and marsviewer [8], were used to display the data.

Testbed data was supplied to the GDS in the same "data product" format as used by MER. This allowed use of the MER telemetry processor unmodified, greatly simplifying the process. Thus the data looked exactly like MER data (except for the spacecraft identifier). Although the RDR generation programs are designed to be easily adaptable to new missions [9], this capability was not needed for the testbed. Generation of EDR's and RDR's was managed by a pipeline nearly identical to the LSOT pipeline [1], which is in turn nearly identical to the MER pipeline [10].

The primary challenge for InSight configured instrument deployment testbed compared with the heritage missions is the lack of a stereo camera. Due to payload volume and mass accommodation constraints there is a single arm-mounted camera. On the Phoenix mission, MIPL demonstrated the capability of doing stereo analysis using an arm-mounted camera (which is very similar in characteristics to the COTS IDA camera) and taking pictures from different points of view. It was a manual process, however, to match images to create stereo pairs. For the InSight configured instrument deployment testbed we solved the problem by marking images as "Left" and "Right" when they were acquired. The stereo pairs were thus determinable by the automated pipeline. In stereo image analysis, knowledge of the baseline (distance between the cameras) is critical. A small error in baseline knowledge is magnified many times (5-6x in analysis conducted for InSight mission concept study). In order to minimize this error, stereo pairs were acquired by moving one arm joint only – the shoulder joint – while keeping all the other joints constant. This worked well, creating terrain models of sufficient quality to support deployment of the instruments. This assignment of images to Left and Right results in a higher data volume, as there is significant overlap between different images. However, the additional accuracy obtained by moving just one joint is a significant benefit, and may outweigh the cost. This is a tradeoff that will be further examined during design and implementation of the actual InSight mission.

Meshes were created from the terrain models using specialized scripts inherited from MER and Phoenix. These meshes were used in the RSVP program to help plan sequences. In the testbed, two types of mosaics were created: workspace mosaics (Figure [13]) and deck mosaics (Figure [14]). Workspace mosaics were a straightforward application of standard MIPL techniques [8].
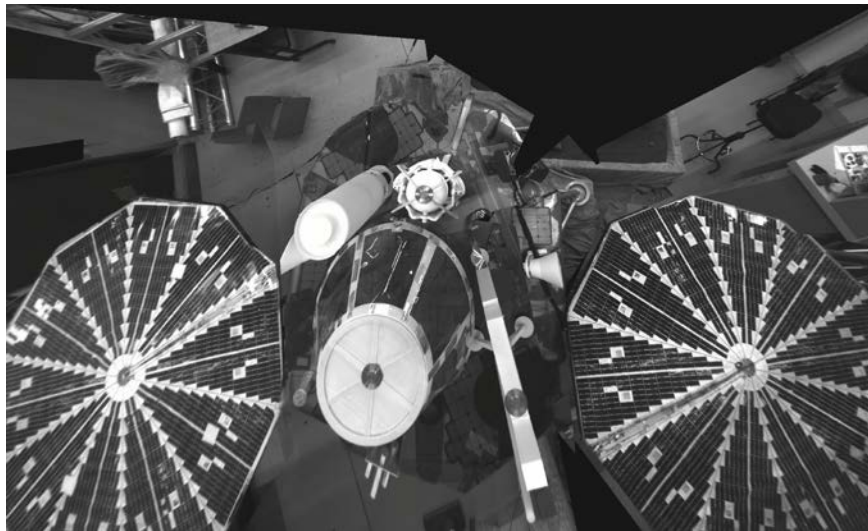
Figure 13 InSight Lander deck mosaic image generated using 10 images.
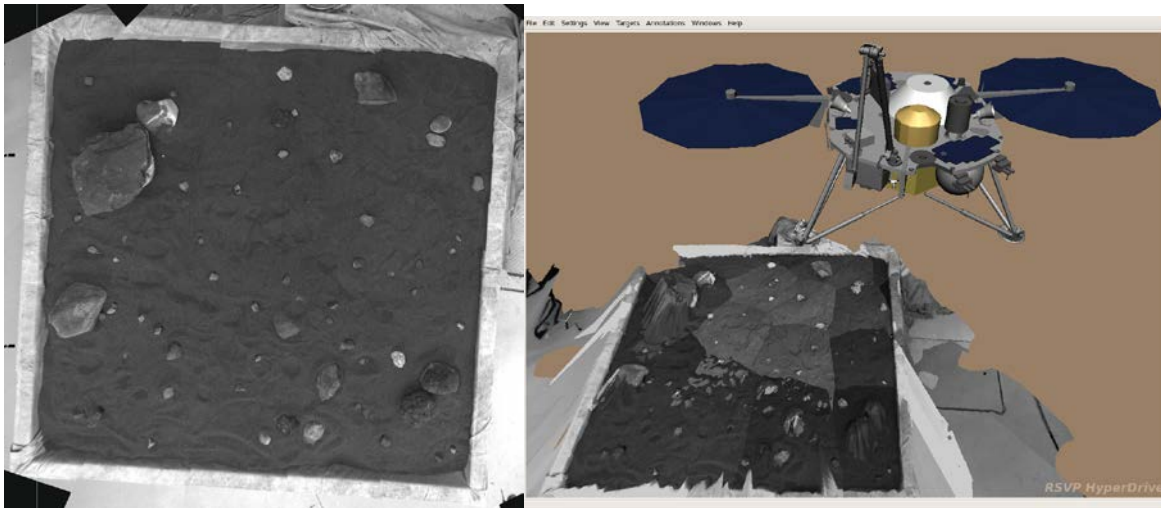

Figure 14 Instrument deployment testbed sandbox mosaic and terrain mesh generated using 17 images.

The deck mosaics, however, were more challenging, due to the extreme parallax involved in looking so close to the camera at a scene with significant depth variations. This parallax causes uncorrectable seams when the edge of a frame intersects an object above the deck. In order to mitigate this, portions of images were masked off in order to shift the seam to the deck itself, thereby eliminating parallax. There is still high distortion in the mosaic due to the parallax, but most of the seams were eliminated, creating a more visually appealing picture. It is likely that the real InSight mission will also take panoramic mosaics of the surroundings, probably after the instruments are deployed. These can be easily dealt with using standard MIPL techniques.

It should be noted that the real InSight mission will require additional adaptation of the MIPL software to make it suitable for the flight mission. Pretending the data is from MER is sufficient for the testbed in order to prove the concepts, but lacks the robustness and flexibility of flight mission support software. The software itself is already flight-mission worthy (having been used extensively for MER, Phoenix, and MSL), but a mission-specific adaptation for InSight will be necessary to capture the details of the mission as built (e.g. telemetry metadata, InSight specific arm kinematics parameters, camera models etc).

Terrain Assessment for Instrument Placement

Inevitably, some areas of the robotic arm's workspace will be more suitable for instrument placement than others. Figure 15 contains the testbed sandbox MIPL composite stereo point cloud color coded for height that illustrates this. Clearly, placing an instrument leg on a rock could increase the risk of instrument tip over. One use of the MIPL 3D stereo reconstruction of the robotic arm's workspace is autonomously identifying the safest patch of terrain in the workspace to place each in situ payload instrument. An InSight Terrain Assessment for Instrument Placement

ground tool was developed to accomplish this. This tool reads in stereo range images generated by the MIPL pipeline of the terrain within the arm's workspace, then generates a high resolution 2.5D elevation map, and searches the elevation map for the safest location to place lander instruments. An in situ payload instrument is virtually placed centered at every cell in the 2.5D elevation map with the instrument legs contacting the terrain map surface. The equation of the plane passing through the bottom of each instrument leg is generated. The equation of the plane is used to determine the tilt of the instrument when placed centered at each cell. Locations with an instrument tilt higher than a user specified threshold are invalid locations. Each range image pixel within the perimeter of the virtually placed instrument is evaluated to determine the maximum terrain relief within the instrument perimeter above the plane through the bottom of the legs. The map location with a valid instrument tilt and the lowest instrument terrain relief is maintained during the search as the safest placement of an instrument. After a search of the map is complete for an instrument and the safest placement for that instrument is found, the map cells within the perimeter of the instrument are flagged as unavailable when evaluating the placement of other instruments. The Insight Terrain Assessment for Instrument Placement software is parameterized. The 2.5D elevation map resolution, minimum and maximum reach of the robotic arm, minimum and maximum azimuth of the robotic arm, maximum tilt of each instrument, and maximum relief of each instrument are all specified in a parameter text file that is read by the software at startup. Figure 16 shows the safest SEIS/WTS and HPS placement in the testbed sandbox as determined by the Terrain Assessment for Instrument Placement tool. Note that these positions are close to the manually selected instrument placement during the site visit, as shown in Figure 17.

High-Fidelity 3D Model Reconstruction for On-Board

Processing

As shown in Figure 9, stereo can be performed between a pair of IDC images with substantial overlay. But there will likely be some loss of data due to inevitable errors in measuring the pose of the camera. The MIPL stereo pipeline results in a high fidelity 3D reconstruction of the imaged scene, but its relatively long processing time makes it most suitable as a ground tool. During the development of the InSight configured instrument deployment testbed, we tested a novel high-fidelity 3D model reconstruction algorithm that performs feature detection and motion estimation prior to applying a newly developed stereo matching algorithm [11].

Feature detection and matching
To establish point correspondences between frames, we used a sub-pixel precise version of the STAR feature detector, a center-surround type detector, for detecting blob-like features [12]. Feature points are matched among frames using an upright version of SURF [13] for efficiency. The

STAR/SURF feature detection and matching provide a good initial translation, rotation and scale between two images. Then they are approximated locally by an affine transform. Finally, we established more accurate point correspondences using the affine transform and a spatial correlation method.

Homography Motion Estimations
A homography is defined by constraining the general rigid body motion equation by a 3D plane equation. Starting from unconstrained point correspondences, we used a RANSAC approach [14] to calculate a homography for the maximum set of matched in-plane feature points for a given reprojection error threshold. This procedure continues until a few point features remained. Then these in-plane features are used for motion estimation by the method suggested in [11]. Because the method in [11] does not estimate the scale factor, we used point correspondences found in more than two images to unify all motion into single coordinate, which in this case is the first frame.

The 3D Model Reconstruction
The motion in previous step was used to construct virtual stereo image pair using the nearby images. We used a newly developed stereo matching algorithm -- Stereo Bias Removal by Autocorrelation (SBRA), to construct a high fidelity 3D model. SBRA can effectively remove stereo biases such as pixel locking and foreshortening errors and improve the 3D model accuracy. This 3D reconstruction procedure is highly automated and fast. For example, the feature selection and matching for a pair of images only takes a few seconds, the motion estimation takes ~20 ms and stereo image matching takes about second. The total image data processing can be done in a few minutes. Figure 18 illustrates constructing a virtual stereo image pair using nearby images. Figure 19 illustrates a high fidelity 3D reconstruction of the testbed sandbox using SBRA. This method could potentially be used to generate a high fidelity 3D reconstruction on-board a lander using images from a single arm camera.
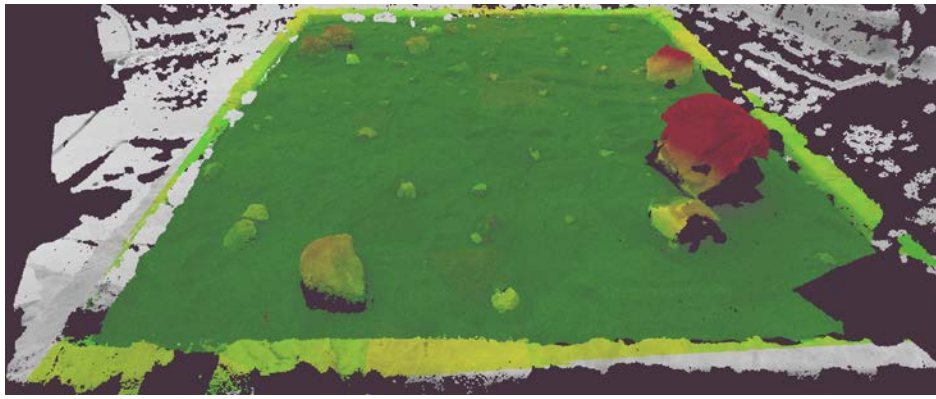
Figure 15 MIPL composite stereo point cloud of the InSight sandbox color coded for terrain height. Green pixels have low elevation and red pixels have large elevation.
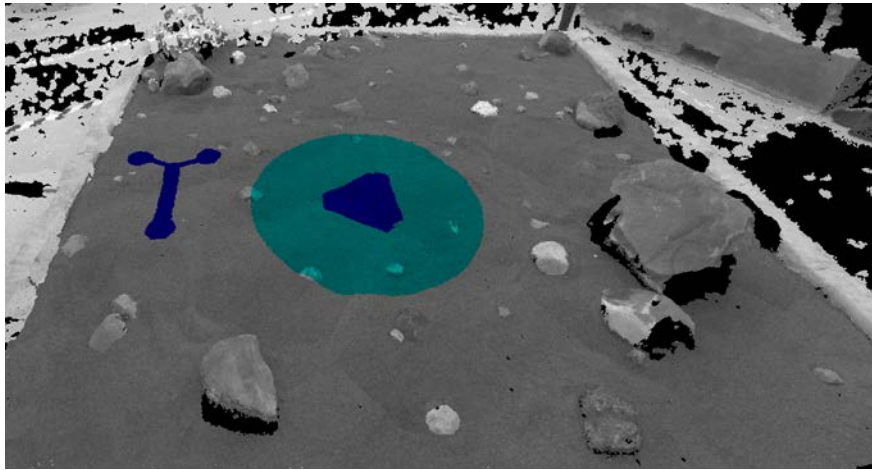

Figure 16 The safest SEIS/WTS and HPS placement autonomously identified using the Terrain Assessment for Instrument Placement tool.

Figure 17 Manually selected SEIS/WTS and HP3 placement during the site visit.

(a) Image at time t	(b) Image at time t+1

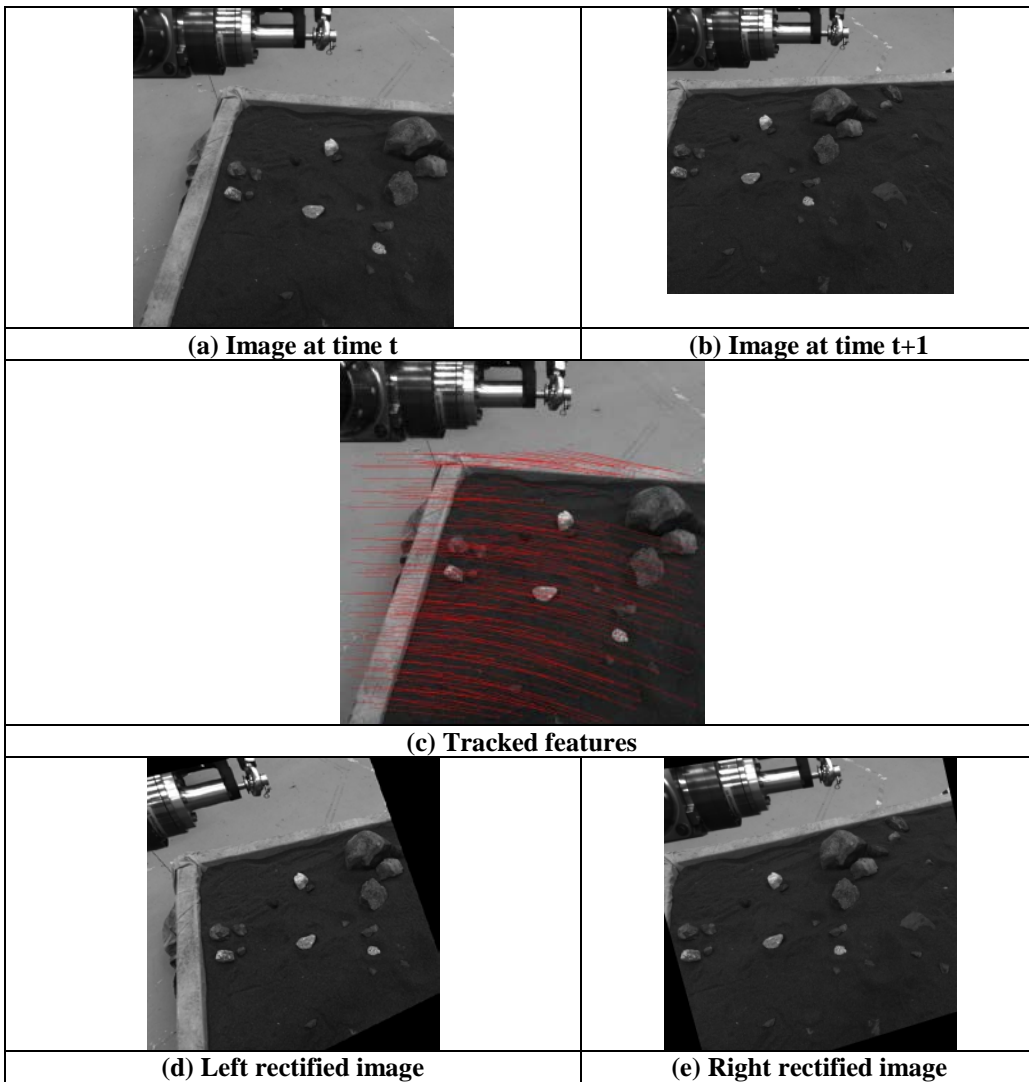| (c) Tracked features | |

| (d) Left rectified image | (e) Right rectified image |

Figure 18 Feature detection and matching is performed between neighbor images. Motion estimation is used to construct a virtual stereo image pair.
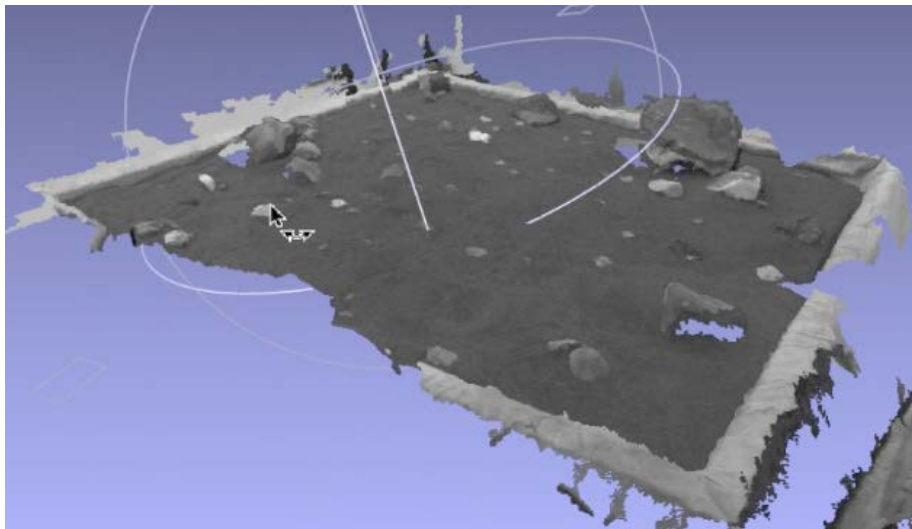

Figure 19 High fidelity 3D reconstruction of the InSight sandbox from processing 40 images SBRA.

3. CONCLUSIONS

The planetary surface geophysics instrument deployment testbed was used extensively in Phase A to perform proof-of-concept testing and demonstrations. The resulting benefits to the project includes: given the integrated team confidence in the feasibility of its development approach; identifying and overcoming hardware design robustness issues such as the selection of the magnetic grapple; help refine flight software and payload requirements; test nominal and fault timelines; help establish preliminary system verification plans; and better evaluate the maturity (TRL) of payload algorithms and hardware.

The planetary surface geophysics instrument deployment testbed was used to successfully demonstrate the end-to-end surfaces operations of the InSight mission to the NASA reviewers at a site visit in May 2012.

In Phase B of the project the instrument deployment testbed will incorporate engineering models of the flight IDS, SEIS, HP3 and IDA workspace models with rocks and regolith simulants, to support development of IDS hardware, procedures, and software. The complete testbed will support deployment-system V&V, and will be incorporated into the project Flight System Testbed at Lockheed Martin in Denver.

Based on our experience developing LSOT and the instrument deployment testbed we have concluded that high fidelity functional "dirty" testbeds provide a cost effective platform for early risk reduction activities and management of risks inherent in complex missions in Phase A of a NASA project life cycle. In addition, to realize the full cost benefits these testbeds should be designed to partial or fully transition to a flight system testbed in Phase B of the project.

REFERENCES

[1] Ashitey Trebi-Ollennu, Khaled S. Ali, Arturo L. Rankin, Kam S Tso, Christopher Assad, Jaret B Matthews, Robert G Deen, Douglass A Alexander, Risaku Toda, Harish Manohara, Mohammad Mojarradi, Michael Wolf, John R Wright, Jeng Yen, Frank Hartman, Robert G Bonitz, Allen R Sirota and Leon Alkalai, "Lunar Surface Operations Testbed (LSOT)," Proceedings of IEEE Aerospace Conference, Big Sky, MT, March 2012.

[2] JPL New Technology Report #48857

[3] Brian H. Wilcox, Todd Litwin, Jeff Biesiadecki, Jaret Matthews, Matt Heverly, Jack Morrison, Julie Townsend, Norman Ahmed, Al Sirota, Brian Cooper, "ATHLETE: A Cargo Handling and Manipulation Robot for the Moon.", Journal of Field Robotics, 2007, Vol. 24.

[4] Reeves, Glenn, "Mars Exploration Rovers Flight Software." Waikoloa : IEEE Conference on Systems, Man and Cybernetics, 2005.

[5] J. Wright, F. Hartman, B. Cooper, S. Maxwell, J. Yen, and J. Morrison, ''Driving on Mars with RSVP,'' IEEE Robot. Automat. Mag., vol. 13, no. 2, pp. 37–45, June 2006.

[6] D. Eisenman, C. Liebe, M. Maimone, M. Schwochert, and R. Willson, "Mars Exploration Rover Engineering Cameras," Sept 2001 SPIE Remote Sensing conference proceedings, Toulouse, France., September 2001.

[7] Rankin, A., Bajracharya, M., Huertas, A., Howard, A., Moghaddam, B., Brennan, S., Ansar, A., Tang, B., Turmon, M., and Matthies, L., "Stereo-vision based perception capabilities developed during the Robotics Collaborative Technology Alliances program," Proceedings of SPIE, Vol. 7692, Orlando, April 2010.

[8] Alexander, D. A., et al. (2006), Processing of Mars Exploration Rover imagery for science and operations planning, J. Geophys. Res., 111, E02S02, doi:10.1029/2005JE002462.

[9] Deen, R. G. (2003), Cost savings through Multimission code reuse for Mars image products, paper presented at 5th International Symposium on Reducing the Cost of Spacecraft Ground Systems and Operations, Deep Space Commun. and Navig. Syst. Cent. of Excellence (DESCANSO), Jet Propul. Lab., Pasadena, Calif.

[10] Alexander, D., P. Zamani, R. Deen, P. Andres, and H. Mortensen (2005), Automated generation of image products for Mars Exploration Rover mission tactical operations, paper presented at 2005 International Conference on Systems, Man, and Cybernetics, Inst. of Electr. and Electron. Eng., Waikoloa, Hawaii.

[11] Cheng, Y., "Stereo Bias Removal by Autocorrelation (SBRA)" Manuscript.

[12] Agrawal, M., Konolige, K., and Blas, M. R., "Censure: Center surround extremas for realtime feature detection and matching.," in [Proc. Europ. Conf. on Comp. Vis.], LNCS 5305, 102–115 (2008).

[13] Bay, H., Ess, A., Tuytelaars, T., and Van Gool, L., "Speeded-up robust features (surf)," Comp. Vis. Image Understanding. 110(3), 346–359 (2008).

[14] Fischler, M. A. and Bolles, R. C., "Random sample consensus: A paradigm for model fitting with applications to image analysis and automated cartography.," Commun. ACM, 381–395 (1981).

Biographies

AshiteyTrebi-Ollennu, FIET, FRAeS, SMIEE *is a technical group leader and robotics software engineer IV of the Mobility and Manipulation group at NASA Jet Propulsion Laboratory, California Institute of Technology, where he has been since 1999. He received his Ph.D. degree in control systems from Royal Military College of Science, Cranfield University, United Kingdom in 1996 and B.Eng. (Hons) from Queen Mary College, University of London, United Kingdom in 1991. Dr. Trebi-Ollennu received the 2008 NASA Exceptional Engineering Achievement Medal for his contributions to the Mars Exploration Rover mission, 2007 Outstanding Engineer Award from IEEE Region 6, 2007 Sir Monty Finniston Achievement Medal from Institution of Engineering and Technology, U.K., and 2010 Specialist Silver Award from the Royal Aeronautical Society, U.K. Dr. Trebi-Ollennu is a Fellow of the Institution of Engineering and Technology, U. K., and a Fellow of the Royal Aeronautical Society, U.K.*

Arturo L. Rankin *is a task manager and robotics software engineer III in the Surface Systems Perception Group at NASA Jet Propulsion Laboratory, California Institute of Technology, where he has been since 1997. He received a B.S. degree in Mechanical Engineering in 1987 from the Catholic University of America, Washington D.C., and M.S. and Ph.D. degrees in Mechanical Engineering in 1993 and 1997 from the University of Florida. Dr. Rankin has developed obstacle detection, terrain perception, and terrain mapping software for a variety of terrestrial and planetary projects. In 2007, Dr. Rankin led an effort that successfully integrated the Field D* global path planner into Mars Exploration Rover flight software.*

Kam S Tso *received his Ph.D. in Computer Science from the University of California, Los Angeles, M.S. in Electronic Engineering from the Philips International Institute, the Netherlands, and B.S. in Electronics from the Chinese University of Hong Kong. Dr. Tso is a member of the Robotics Modeling, Simulation, and Visualization Group at JPL. He has worked on a variety of robotics research projects including the JPL Telerobot, Remote Surface Inspection, Web Interface for Telescience, and Lunar Surface Operations Testbed. He is currently the software lead of the GEMS Payload Testbed. His research interests include visualization and simulation, robotics, cyber security, high performance and dependable real-time software and systems.*

Dr. Yang Cheng *is a senior member of the Aerial Perception Group at Jet Propulsion Laboratory (JPL), where he is developing vision algorithms for planetary spacecraft. He is a key developer of numerous computer vision modules for spacecraft autonomous navigation and landing, such as the crater landmark detection/matching algorithm for spacecraft localization, the Descent Image Motion Estimation System (DIMES) for Mars Exploration Rover (MER) landing, MER visual odometry, Rock detection and Mapping for Phoenix lander etc. He is co-PI for computer vision algorithms for a Phase A & B study of Terrain Relative Guidance System for the NASA New Millennium program. Currently, he is working on terrain relative navigation (TRN) system for future PPL missions.*

Eric A. Kulczycki *received a dual B.S degree in Mechanical Engineering and Aeronautical Science and Engineering from the University of California, Davis, in 2004. He received his M.S. degree in Mechanical and Aeronautical Engineering also from the University of California, Davis in 2006. He is a member of the engineering staff at the Jet Propulsion Laboratory, California Institute of Technology, where he is currently involved in atmospheric sample collection, comet sample return capture systems, dynamic modeling of ground vehicles, and mechanical design of various mobility platforms. He has worked at JPL for over 10 years.*
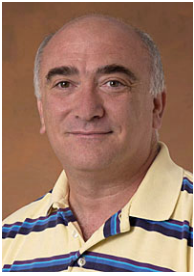
Hrand Aghazarian *received his M.S. in Computer Science, and dual B.S. in Computer Science/Applied Math California State University, Northridge, CA. Hrand is member of Robotic Software Systems Group at JPL. He has worked on variety of robotics research projects including wheeled, legged, under-water and surface boat robotics. His research interests include Single/Multi Robot Control, Robotics Software Architecture, Obstacle Avoidance, Genetic Algorithm, and Path Planning.*

`Robert G. Deen` *received a B.S. degree (with honors) in computer science from Texas A&M University (College Station) in 1987. Since then he has worked at the Multimission Image Processing Laboratory of the Jet Propulsion Laboratory in Pasadena, CA, where he is a Principal Software Engineer. His primary duties include responsibility for the ground-based image processing software used for in-situ mission operations and science, including the Mars Exploration Rovers (MER), Phoenix, and Mars Science Laboratory (MSL).*

Robert G Bonitz *is a principal engineer with the Mobility and Manipulation Group at the Jet Propulsion Laboratory. He was the Phoenix Lander 2007 Robotic Arm Manager. Previously he developed the control algorithms and software for the Mars Exploration Rover and Mars Polar Lander robotic arms. He has conducted research in control algorithms for multiple-manipulator robotic systems, robust internal force-based impedance controllers, frameworks for general force decomposition, optimal force control algorithms, and calibration methods for multi-arm robotic systems. He has worked for a variety of industrial companies including Raytheon, TRW, Source 2 International, and GTE. He has a Ph.D. in Electrical Engineering from the University of California, Davis.*
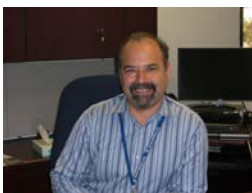
Leon Alkalai *, (Member of IAA), is the Program Manager of the JPL Lunar Robotic Exploration Program Office in the Solar System Exploration Directorate (4x) and the Capture Lead for the Mars GEophysical Monitoring Stations (GEMS) proposal to the NASA Science Mission Directorate (SMD) Discovery Program which was recently selected for a Phase A study. For the last seven years, he has led JPL's lunar robotics mission formulation efforts for both SMD and ESMD, including the Gravity Recovery And Interior Laboratory (GRAIL) mission which won the last Discovery Program competition. Leon was also the formulation lead for the MoonRise Lunar Sample Return mission from the South Pole-Aitken Basin, Phase A study. Prior to transitioning his career at JPL to mission formulation, he worked at JPL for 14 years in the technology development and technology management areas including the Center Lead for the Center for Integrated Space Microsystems. Leon received his PhD from UCLA in 1989 and since then has worked at JPL. He is an Adjunct Faculty at UCLA Computer Science Department, a Full Member for the International Academy of Astronautics (IAA), and the Chief Technologist for the National Space Biomedical Research Institute (NSBRI).*